Optimization of random searches on defective lattice networks

M. C. Santos,[1] G. M. Viswanathan,[2] E. P. Raposo,[3] and M. G. E. da Luz[1,*]
[1]*Departamento de Física, Universidade Federal do Paraná, 81531-990 Curitiba-PR, Brazil*
[2]*Instituto de Física, Universidade Federal de Alagoas, 57072-970 Maceió-AL, Brazil*
[3]*Laboratório de Física Teórica e Computacional, Departamento de Física, Universidade Federal de Pernambuco, 50670-901 Recife-PE, Brazil*
(Received 30 November 2007; published 2 April 2008)

We study the general problem of how to search efficiently for targets randomly located on defective lattice networks—i.e., regular lattices which have some fraction of its nodes randomly removed. We consider large but finite triangular lattices and assume for the search dynamics that the walker chooses steps lengths ℓ_j from the power-law distribution $P(\ell_j) \sim \ell_j^{-\mu}$, with the exponent μ regulating the strategy of the search process. At each step ℓ_j, the searcher moves in straight lines and constantly looks within a detection radius of vision r_v for the targets along the way. If there is contact with a defect, the movement stops and a new step length is chosen. Hence, the presence of defects decreases the efficiency of the overall process. We study numerically how three different aspects of the lattice influence the optimization of the search efficiency: (i) the type of boundary conditions, (ii) the concentration of targets and defects, and (iii) the category or class of search—destructive, nondestructive, or regenerative. Motivated by the results, we develop a type of mean-field model for the problem and obtain an analytical approximation for the search efficiency function. Finally we discuss, in the context of searches, how defective lattices compare with perfect lattices and with continuous environments.

DOI: 10.1103/PhysRevE.77.041101 PACS number(s): 05.50.+q, 89.75.Fb, 05.40.−a, 89.75.Da

I. INTRODUCTION

How does one optimize the search in continuous disordered media, where the location of the target objects are not known *a priori*? This problem of finding, in the most efficient way, randomly distributed target sites has attracted interest in several areas of research [1,2]: e.g., (i) the modeling of foraging processes [3–13] by diverse animal species in theoretical ecology, (ii) oil recovery from mature reservoirs in geology [14], (iii) studies of dynamics at the extinction edge in scenarios of low availability of energetic resources [15], and (iv) automated computer searches of registers in high-capacity databases [16] in information technology. In the majority of such examples, the random searches are performed in an Euclidean environment. Nevertheless, in digital spaces and in concrete physical lattice networks (see below), the search takes place in discrete topologies.

Lattice models have yielded important results for the understanding of complex systems phenomena: e.g., neural processing [17–19] and dynamics of computer [20,21] and social [22] networks [23,24]. Because of their fundamental and practical relevance, it is natural to extend the above initial question to searches in discrete landscapes. In this context many studies [23,25,26] have reconfirmed the hypothesis that the topological features of the lattices, especially site connectivity, do indeed affect the transport of information.

In particular, regarding the above latter aspect, works in the literature [27] address the properties of a lattice when defects (breakdowns via removal of bonds or nodes) are introduced, e.g., the instability of the network with the destruction of "hubs," the routing determination when the lattice connectivity is time dependent as in peer-to-peer (P2P) networks, etc. However, the influence of such random "dilution" on the efficiency of random searches has not yet been thorough analyzed. Potentially, this study could be useful to solve a variety of problems, such as how to find stretches of information in a computer storage device which is partially damaged or how to randomly look for a gas station in an unfamiliar city during rush hour, when the streets are jammed.

In general, networks can be classified into two large classes of systems: (i) large-world networks and (ii) small-world networks. Large-scale networks are locally connected and rich in clusters, with only short-range links, basically between first-neighbor sites. In such cases, the distribution of link sizes is a narrow Gaussian, truncated close to the origin, giving rise to a linear increase of the mean distance between two arbitrary sites (lattice diameter) with the total number of sites [25,28]. These networks have been associated with low efficiency of transport properties [25] and typically can be modeled by two-dimensional (2D) regular lattices with defects. In contrast, small-world networks are globally connected and highly efficient for transport. They possess power-law link distance distributions. Furthermore, their topologies reveal cluster formation associated with the large number of local links [25]. The lattice diameter grows sublinearly (logarithmically) [25,28] with the number of sites due to the existence of rare long-range links—the ultralong links act as shortcuts that reduce the number of links necessary across which the information must propagate (an example being the World-Wide Web [29]).

While discussions on the optimization of high-performance small-world networks are numerous [23,26,30,31], studies dealing with the efficiency of large-world networks are far less common [32]. Nevertheless, optimizing the search in inefficient networks, including large-world networks, is an equally important problem. For instance, it relates to situations of very high cost for transforming the link configuration from a large-world one to

*luz@fisica.ufpr.br

small-world one [33]. Moreover, a really large number of concrete situations of interest [34] are in their essence large-world networks, characterized by structures that have only first-neighbor links between the lattices nodes and which cannot be physically modified. A nice example is the traffic system in small- and medium-size towns [35]. Finally, even if the topology of a lattice is of small-world kind, yet some of its features may be better associated with a large-world topology. Indeed, a great variety of biological networks are typically scale free [36]. But in some instances, like in gene networks [37], many of the links are so weakly related—with respect to a particular functionality—that they can be neglected without important modification for the dynamical response of that functionality, effectively leading to a large-world problem.

Therefore, as a first step toward understanding the random search features in defective large-world networks, here we adapt a search model, already successfully applied to continuous spaces [9], to the case of discrete fragmented environments, created by removing a certain number of nodes of originally regular triangular lattices. We consider then a random walk with step lengths chosen from an asymptotic Lévy distribution $P(\ell_j) \sim \ell_j^{-\mu}$. At each step j the walker moves in straight lines along the directions allowed by the lattice with defects, constantly looking for target sites along the way. Different values of μ set the different strategies of the search. We should observe that for the particular case of defect-free regular lattices, this type of analysis has recently [32] led to some interesting results, revealing how distinct strategies should be chosen so as to optimize the random search depending on the various features of the regular lattice, such as topology and type of boundary conditions.

The article is organized as follows. In Sec. II we introduce aspects of defective lattices and the search model procedure. Results and discussion of the numerical simulations are presented in Sec. III, where an analytical model is also developed. Final remarks and conclusion are drawn in Sec. IV.

II. MODEL

A search process is fully characterized once one establishes the following: (i) the features of the search space and (ii) the strategy adopted to find the targets. We next discuss these two aspects of the model.

A. Lattice properties

We begin by analyzing the search environment and its properties—mobility and connectivity. We assume a two-dimensional lattice, with lattice constant $s=1$. Each node connects to its nearest neighbors in a triangular topology (see Fig. 1). We consider three types of boundary conditions: periodic (PBC), helical (HBC), and wall (WBC), respectively, Figs. 1(a), 1(b), and 1(c). The importance of boundary effects in the present context arises due to the fat-tailed step distribution and to the finite size of the lattices. Actually, the combination of both factors might enhance the probability of a given search walk to reach the lattice boundaries, depending on the set of parameters considered (see discussion on specific cases below). Note also that the BC choice is not relevant for Brownian walks in lattices of sizes much larger

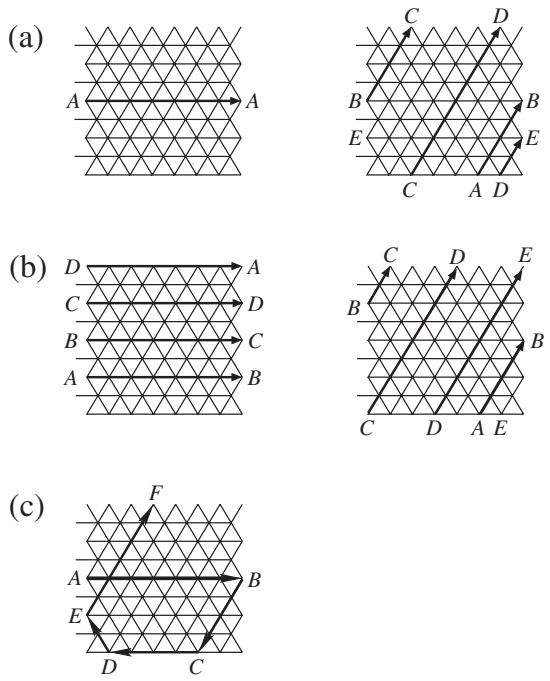

FIG. 1. Illustration of the triangular lattice and its boundary conditions: (a) periodic; (b) helical; and (c) not specular wall.

than the first and second momenta of the step distribution, but it turns to be definitively important, even in very large discrete lattices, when the distribution considered presents huge (diverging) momenta.

Regarding specific aspects of the BCs studied in this work, we first observe that the PBC leads to a torus lattice. In this case, horizontal paths [Fig. 1(a), left] are closed circles, whereas diagonal paths [Fig. 1(a), right] form solenoidlike curves. Indeed, note that the trajectory *ABCDE*… in the figure is not closed until all the nodes are visited. Moreover, the HBC differs from the PBC because the left is connected to the corresponding right border shifted by one node [Fig. 1(b), left]. A similar relation holds for the top and bottom boundaries [Fig. 1(b), right]. This shifting generates a twisted torus lattice. Therefore, the horizontal paths create a solenoid that is closed after half of the nodes are visited. The diagonal paths also create a solenoid, which, analogously to the PBC case, closes only after visiting all nodes. Finally, in the WBC any node along the boundary acts like a hard wall, but not specularly. Thus, any path hitting a border node becomes truncated and a new path, having a direction which is randomly chosen, must begin.

To create defects, diluting the network, we randomly eliminate a certain fraction of nodes from an initially regular lattice. If we denote by n_0 the initial number of nodes in a perfect lattice, the *fragmentation coefficient* is defined by $\chi = n_d/n_0$, where n_d is the total number of nodes removed. Examples are given in Fig. 2. Note that $\chi=1$ implies an empty space—total dilution, complete destruction of the lattice. The mean number of connections per node, k_f, reduces linearly as χ grows according to $k_f=(1-\chi)k$, with $k=6$. Note that $k=6$ is the number of first neighbors in a triangular lattice without defects ($\chi=0$).

Relevant for the present random search problem is to understand how the increase of defects—i.e., variation of

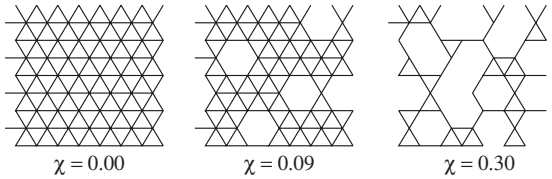

FIG. 2. Examples of a perfect ($\chi=0$) and two defective lattices. Here $n_0=56$.

χ—alters the mobility and connectivity in the lattice. We address this question by assuming a lattice with $n_0=4\times10^6$ and study two useful quantities.

First, we assume a random walk, whose step lengths ℓ_j are given by the distribution $P(\ell_j)\sim\ell_j^{-\mu}$ with $\mu=1.1$, which represents nearly ballistic steps. We also impose a maximum value for ℓ_j (an upper cutoff) of $\ell_{\max}=\sqrt{n_0}=2\times10^3$. We use PBC, but due to the chosen cutoff, the exact boundary conditions are not very important here. A full run stops after traveling a total distance $L=n_0=4\times10^6$ along the lattice. Then, we consider the initial perfect lattice divided into 100 regions (quadrants), all having the same number of nodes. Next, for a given value of χ we implement $N=100$ different realizations and for each perform the mentioned random walk. Finally, we compute $\sigma(\chi)$, which gives the fraction of quadrants visited by the walker at least once in a run (averaged over such $N=100$ runs). The results, displayed in Fig. 3(a), show that only for low fragmentation ($\chi<0.1$) does the coefficient σ remain close to unity, so that all the quadrants are still available to the walker and, on average, the whole lattice can be accessed starting from any arbitrary site. Above a critical value for the number of defects one has $\sigma=0$, indicating that the lattice is critically disconnected and that leaving the initial quadrant becomes a rare event. It is interesting to note that such a critical fragmentation coefficient for the mobility measure, $\chi_c\approx0.5$, coincides with the triangular lattice percolation threshold [38]. So, as it should be, the fraction of visited quadrants by a random walker is directly connected to how close the defective lattice is to its percolation limit. In fact, observe a rapid reduction of the mobility ($\sigma\to0$) in the range $0.2<\chi<0.5$. However, as we are going to discuss in Sec. III A, for Lévy or any other random strategy to effectively improve the efficiency of a search, the concentration of defects in a regular lattice cannot be too high. Thus, in our analysis we will be relatively away from the threshold of the associate percolation problem.

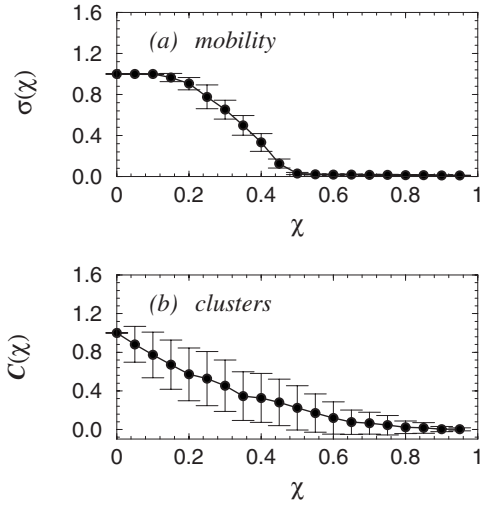

FIG. 3. (a) Fraction of quadrants visited at least once by a random walker and (b) coefficient of cluster formation (which measures the average number of first neighbors of the nodes), as functions of the fragmentation coefficient χ.

A second interesting function is the coefficient of cluster formation, $C(\chi)$, which we adapt from Ref. [25]. It is defined as the following. Take an arbitrary node s, with k_s closest neighbors. Then, at most $k_s(k_s-1)/2$ connections could be formed between them (when all the neighbors of s are also connected to each other). We assume that, if connected, two nodes are joined by only one bound. Then, C_s represents the proportion of these possible connections which indeed exists. C is just the average of C_s over s. For the above lattice parameters and again for 100 realizations for each χ, we show in Fig. 3(b) the numerically calculated $C(\chi)$. We clearly see that the defects lead to a rapid break up of the clusters.

B. Random search rules

For the random search process, we assume that the target sites are distributed randomly at the nodes of the lattice, giving a total number of $n_t\leq n_0-n_d$. We classify the target sites as follows: destructive (i.e., perishable), which become irreversibly unavailable for future visits once found by the searcher; nondestructive (i.e., nonperishable), which can be revisited an arbitrary number of times; and finally, an intermediate case of regenerative targets; i.e., once found, they become again accessible after a finite recovery time. To assure stationarity also in the destructive case [9,15,32], yet keeping the expected results for a destructive process [39], a new site is randomly placed every time a target site is found and destroyed.

The searchers perform random walks, whose step lengths ℓ_j are distributed according to (with $\ell_j>\lambda_0$, for λ_0 a lower cutoff)

$$P(\ell_j)\sim\ell_j^{-\mu}. \tag{1}$$

Sums of such steps converge to the long-distance regime of the Lévy-stable distribution [40–44], with Lévy index $\alpha=\mu-1$, for $1<\mu\leq3$. The Brownian behavior corresponds to the case $\mu\geq3$ [45,46]. In the interval $1<\mu<3$, the step lengths ℓ_j do not have a characteristic scale, lower moments diverge, and the distribution acquires self-affine properties—i.e., $P(\gamma\ell_j)\sim\gamma^{-\mu}P(\ell_j)$. The exponent μ determines the features of the search walk: almost rectilinear or ballistic ($\mu\to1$), Brownian ($\mu\geq3$), and superdiffusive ($1<\mu<3$).

We consider the following rules for the search model.

(A) The orientation in each step j is randomly chosen from one of the six possible directions along the lattice.

(B) The step lengths ℓ_j are taken from the distribution (1), where an upper cutoff $\ell_{\max}$ is imposed to the values of the ℓ_j's.

(C) While traveling the distance ℓ_j, the searcher constantly looks for target sites within the closest r_v neighbors of

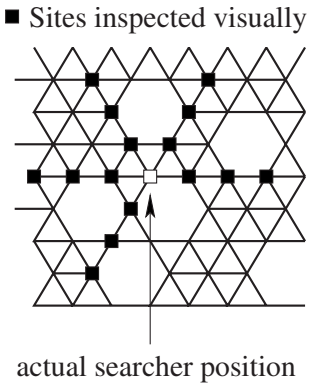

FIG. 4. Schematic representation of the visual inspection rule (C). Only sites at most a distance r_v along the lattice directions are directly visible to the searcher. Here $r_v=3$.

its present location (see Fig. 4). So r_v is a "vision" radius of detection. If a target site is detected, the searcher moves straightforwardly to it and the step is truncated.

(D) If a defect exists along the step j direction (within the distance ℓ_j) and no target sites are found before reaching it, the step is truncated at the node just before such defect.

(E) If truncation events (C) and (D) do not occur, then the searcher proceeds until traversing the distance ℓ_j.

(F) After any of the cases (C), (D), or (E), the process resumes in (A). The walk ends when the searcher traverses an established total distance L.

We characterize the performance of the random search process through the efficiency function $\eta(\mu)\equiv Q/L$. Here, Q is the total number of target sites found after traveling the distance L. We numerically calculate the quantities of interest by averaging over $N=100$ simulation runs. Finally, since we want to explicitly see the influence of the boundary conditions, unless otherwise mentioned we always assume the very large value of $\ell_{\max}=10^{15}\gg\sqrt{n_0}$.

III. RESULTS AND DISCUSSION

In the studied model of random search in lattices with defects, there are many features determining the process efficiency. For clarity, we present our discussions according to different aspects influencing it.

A. Truncation of the Lévy steps

During the walk, the searcher uses the distribution (1) as the metric associated with the step length. At any step j, ℓ_j shorter than λ_0 is rejected. Note that for a random search on a perfect lattice, one should have $\lambda_0\geq r_v$, since any target site located at a distance shorter than r_v is directly accessed according to rule (C) above. On the other hand, statistically, long steps are truncated on average at a distance λ, associated with the free mean path, which depends on the radius of vision, r_v; the number of target sites, n_t; and the number of defects, n_d. The ratio λ/λ_0 gives then an effective dimensionless characteristic size of the dynamical process. Observe that it decreases with the increase of r_v, n_t, and n_d since then the probability of truncation by finding either a target site or a defect is enhanced. In particular, if r_v is of the order of the mean distance λ_t between target sites, one has $\lambda/\lambda_0\approx 1$, indicating that it is not necessary to look for a target site since one of them can always be found nearby. Thus, each step is truncated. An analogous situation occurs when the lattice is relatively well populated by defects ($\chi>0.2$), with a small mean distance between them ($\lambda_d\approx\lambda_0$), implying $\lambda/\lambda_0\approx 1$. The relations between λ and λ_0 and the system parameters are

$$\lambda_0\equiv\frac{n_d+2r_v^2n_t}{n_d+2r_vn_t},\quad \frac{\lambda}{\lambda_0}=\frac{n_0}{n_d+2r_v^2n_t}. \tag{2}$$

We leave to Sec. III D the appropriate justification for these expressions.

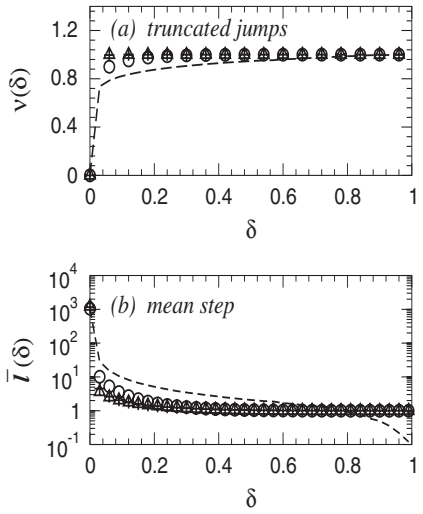

FIG. 5. (a) Fraction $\nu(\delta)$ of truncated steps. (b) Average step length $\bar{l}(\delta)$. The dashed line represents the random walk on a fragmented lattice (for which $\delta=\chi=n_d/n_0$). For the random searches on a perfect lattice (for which $\delta=n_t/n_0$), r_v is equal to 1 (circles), 3 (crosses), and 5 (triangles). The other parameters are specified in the main text.

Next, we shall illustrate how the step lengths of a searcher are truncated on a perfect lattice with target sites and on a defective lattice with no target sites. In the first case the walker effectively performs a random search and in the second it is just a random walker [subjected to the defect-induced truncations, rule (D)]. For the former (latter) situation we define $\delta=n_t/n_0$ ($\delta=\chi=n_d/n_0$). As concrete examples, we set the parameters $n_0=4\times10^6$, PBC, $L=2\times10^7$, $\mu=1.1$, and consider nondestructive searches for three different values of r_v: namely, 1, 3, and 5. We also impose the upper cutoff $\ell_{\max}=\sqrt{n_0}$ for the step lengths, once here we shall avoid the effects of loops in the lattice. Observe that this cutoff is not relevant when $\delta\geq 1/\sqrt{n_0}$, because then on average there is at least one target site or defect in each lattice line, so necessarily every step larger than the lattice size will be truncated.

In Fig. 5 we display two different quantities obtained from the above described simulations. The first is the average fraction of truncated steps in a run, ν, as a function of δ, Fig. 5(a). The second is the actual average step length $\bar{l}(\delta)$, shown

in Fig. 5(b). Both the pure random walk and the random search present a fairly global qualitative agreement (for δ being n_d/n_0 in the former and n_t/n_0 in the latter). Note that even for small values of δ in the two cases, the average step length is very short compared to the lattice side $\sqrt{n_0}$, Fig. 5(b). This is not a surprise because already for $\delta \approx 0.1$, about 80% of the steps are truncated as seen in Fig. 5(a). The only difference of behavior is observed for $\bar{l}(\delta)$ when δ is close to 1. But this is straightforward to understand. In the pure random walk, the limit $\delta \to 1$ means that there is no more lattice. So for $\delta \approx 1$ the great majority of the nodes are isolated, rendering the walker to stay trapped at its present node and hence $\bar{l} \approx 0$. Nevertheless, in the random search, δ around the unity means that the lattice is saturated with targets, so the steps always truncate after one lattice parameter $s=1$.

Based on the previous discussions, we point out the following. When $\lambda/\lambda_0 \approx 1$, regardless the μ, the search space only allows steps of lengths around $\lambda \approx \lambda_0$ and the distribution of effective steps has mean value λ, for destructive and nondestructive searches. Therefore, the limit $\lambda/\lambda_0 \approx 1$ is trivial since the effective walk is certainly Brownian and the efficiency $\eta(\mu)$ remains invariant with respect to the search strategy. In order to avoid this simple regime, in our study next we adjust $r_v \ll \lambda$ and restrict the concentration of target sites and defects to no more than 10%. So, relatively below the percolation threshold $\chi_c \approx 0.5$ seen in Sec. II A.

B. Boundary conditions and the average truncated step length $\bar{l}$

For finite lattices, the exact nature of the boundary conditions can play an important role in the efficiency outcomes of a random search. But this is true only when the search trajectories reach the lattice limits with a certain frequency, which is the case when typically $\lambda/\lambda_0 > \sqrt{n_0}/(10\lambda_0)$ (hereafter called regime I). Here we study the different influence of three types of boundary conditions in the mean-free-path regime I: periodic (PBC) [Fig. 1(a)], helical (HBC) [Fig. 1(b)], and wall (WBC) [Fig. 1(c)]. We consider nondestructive search, $\mu=1.1$, $r_v=1$, $n_0=4\times10^6$, and $n_d=10^3$. The change in λ/λ_0 is obtained by varying n_t from 1 to 4×10^5. Finally, as the total distance to end each simulation run, we set $L=2\times10^5\lambda$.

The PBC makes the lattice a torus, allowing looplike circular trajectories. When confined in one of these loops, without target sites or defects to stop the loop, the searcher necessarily traverses the whole step distance ℓ_j with no truncation. In such cases, arbitrarily long steps (up to $\ell_{\max}$) are allowed. As a consequence, we expect the search efficiency to decrease as μ is lowered from 2 to $1+\epsilon$ (ϵ very small, but not 0 because normalization), in both destructive and nondestructive cases (see Secs. III C and III D). A related behavior is already seen in plots of the mean step length $\bar{l}$ as a function of λ/λ_0. Indeed, for the nondestructive case and PBC, we display in Fig. 6 (circles) the very fast increasing of $\bar{l}$ for large values of λ/λ_0.

The HBC transforms the lattice into a twisted torus with solenoidal trajectories. So loops do not occur, and hence such topology allows a more efficient search than the PBC case. However, note that the search paths form a kind of coil spring and, thus, even very long steps may inspect only a relatively small part of the lattice. Moreover, a very long horizontal step can cover at most half the lattice. As a consequence, we can have a considerable number of steps ℓ_j truncated to values larger than λ, but still much shorter than the upper cutoff limit $\ell_{\max}$. Thus, the variation of $\bar{l}$ with λ/λ_0 is relatively slow, with no abrupt changes as for the PBC. Indeed, compare the two cases in Fig. 6.

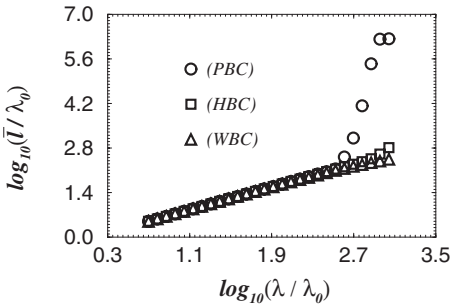

FIG. 6. Mean step length $\bar{l}(\lambda/\lambda_0)$ for nondestructive search. The variation in λ/λ_0 is obtained by changing only the number of target sites n_t. Notice the rapid increasing of $\bar{l}$ for PBC. This is not the case for HBC and WBC.

Lastly, the WBC does not generate loops and produce search paths which are much more ergodic than those for PBC and HBC [indeed, compare Fig. 1(c) with Figs. 1(a) and 1(b)]. Therefore, such paths results in truncations for step lengths of the order of λ. This is displayed in Fig. 6, where for $\log_{10}[\lambda/\lambda_0] > 2.7$, although yet not very pronounced, we start to see some difference between the mean step length $\bar{l}$ of the HBC and of the WBC.

In summary, the initially chosen ℓ_j step lengths can be truncated either because the walker finds a target or it hits a defect. For regime I, the different boundary conditions set different values for the maximum truncated distance d, which effectively can be traveled during a single step. They are listed in the first row of Table I.

C. Target density regimes and the efficiency function $\eta(\mu)$

The shape of the efficiency curves are strongly influenced by the truncation of Lévy steps. We therefore classify the results of search optimization into four regimes. As already mentioned, regime I occurs when the boundary conditions

TABLE I. For different λ/λ_0 regimes and boundary conditions, the effective larger distances d that the walker can move in a single step due to the steps ℓ_j truncation mechanisms.

Regime	PBC	HBC	WBC
I	$d \approx \ell_{\max}$	$d > \lambda$	$d \approx \lambda$
II	$d \approx \lambda$	$d \approx \lambda$	$d \approx \lambda$
III	$\lambda_0 \lesssim d \lesssim 10\lambda_0$	$\lambda_0 \lesssim d \lesssim 10\lambda_0$	$\lambda_0 \lesssim d \lesssim 10\lambda_0$
IV	$d \approx \lambda_0$	$d \approx \lambda_0$	$d \approx \lambda_0$

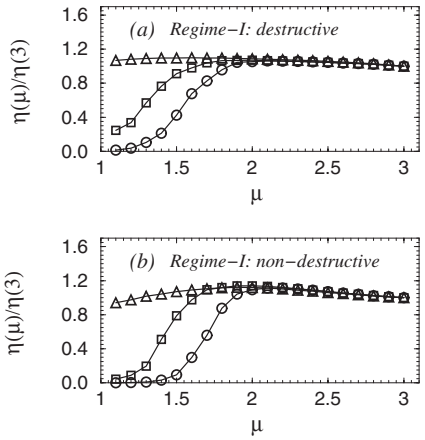

FIG. 7. The normalized efficiency $\eta(\mu)/\eta(3)$ as function of μ for (a) destructive and (b) nondestructive searches. The parameters values (main text) characterize regime I. For the PBC case (circles) $\eta(\mu\to 1)\to 0$ due to the existence of loops. Even without developing loops, the lower scanning power of the HBC (squares) also leads η to decrease for smaller μ. The best overall efficiency is presented by the WBC (triangles).

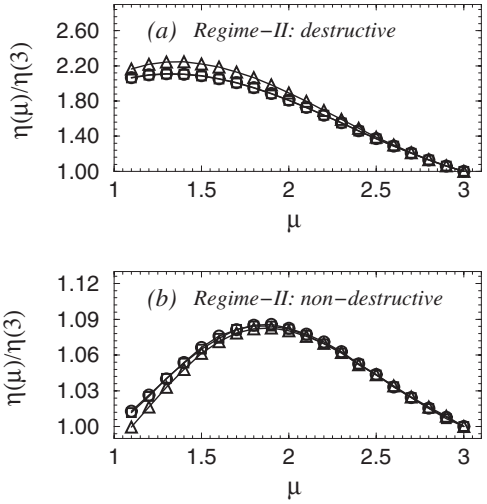

FIG. 8. As in Fig. 7, but for regime II and parameters given in the main text. Note that the curves for distinct boundary conditions overlap, indicating that in regime II the difference between PBC (circles), HBC (triangle), and WBC (squares) is not very important.

are determinant: namely, $\lambda/\lambda_0 > \sqrt{n_0}/(10\lambda_0)$. In this case, truncations of the step lengths $\ell_j \leq \lambda$ (with the exception of the WBC) are not frequent. On the other hand, an intermediate situation for which $10 < \lambda/\lambda_0 < \sqrt{n_0}/(10\lambda_0)$ (regime II) is characterized by a high truncation rate, making the borders of the lattice rarely accessible to the searcher at a single step. Thus, the efficiency function $\eta(\mu)$ is almost independent of the particular boundary condition. As in regime III we assume $1 < \lambda/\lambda_0 < 10$, close to the saturation, but still demanding from the searcher a small number of steps (of order of few lattice parameter s) to find a target site. Finally, regime IV is the complete saturated case—all steps are truncated due to near-maximum site occupancy by targets. The effective larger distance d for all regimes are listed in Table I.

In regime I, where steps truncations are not frequent, each type of boundary condition has a peculiar influence for both destructive and nondestructive efficiency function. For this regime, in Fig. 7 we show $\eta(\mu)$ [normalized by the Brownian efficiency $\eta(3)$] considering the parameters $r_v=1$, $n_0=4\times 10^6$, $n_t=10^3$, $n_d=10^3$, $\lambda/\lambda_0=1331.33$ [from Eq. (2)], and $L=10^5\lambda$. Usually, a destructive search favors ballistic long-step strategies for there is no reason to remain close to a visited site. This is fairly the case for the WBC, for which η increases around 10% from $\mu=3$ to its maximum value at $\mu\approx 1.5$. However, the existence of loops for the PBC and a "weaker ergodicity" of the HBC (see the discussion in the Sec. III B) lead to low efficiency if $1<\mu<2$. So one finds $\eta\to 0$ for $\mu\to 1$ in these two cases. On the other hand, Brownian strategies ($\mu\geq 3$) give the same results for all boundary conditions. Furthermore, generally $\eta(\mu\geq 3)$ is lower than $\eta(\mu\approx 2)$ since the searcher tends to keep close to the last visited and destructed site, with the nearest target site available only after a large number of small steps in the case of low and intermediate concentrations of target sites. These observations are summarized in Fig. 7(a), which displays $\eta(\mu)$ for a destructive search. Note that for the WBC $\mu_{opt}\approx 1.4$, but the efficiency is almost the same for smaller values of μ. In the case of HBC and PBC they are, respectively, $\mu_{opt}\approx 1.8$ and $\mu_{opt}\approx 2.0$.

For the nondestructive search, we observe that $\mu_{opt}\approx 2$ in any of the boundary conditions, Fig. 7(b). This strategy represents a compromise between the importance of long versus short steps, as it can be advantageous to stay near a previously visited site, always visitable again, but also to move ballistically to look for distant sites. In spite of this compromise, the loops in the PBC reduce drastically the efficiency of superdiffusive strategies with $1<\mu<2$, observed directly in the plot. This results in $\eta(\mu)\to 0$ when $\mu\to 1$. Note that the peak at μ_{opt} for the WBC efficiency is not so pronounced when compared with the whole curve, as seen for the other two boundary conditions by confronting $\eta(\mu_{opt})$ with η for small μ's. We also mention that although the local dynamics of destructive and nondestructive searches are rather distinct, in this regime I their curves $\eta(\mu)$ turn out to be very similar. Finally, we stress that if we plot the $\eta(\mu)$ of Fig. 7 without any normalization, as expected we find that the WBC always presents the best efficiency for all μ's.

For regime II, we plot the efficiency function in Fig. 8 using the parameters values $r_v=1$, $n_0=4\times 10^6$, $n_t=8\times 10^3$, $n_d=10^4$, $\lambda/\lambda_0=153.61$, and $L=10^5\lambda$. In the destructive case, the distribution of defects and sites implies in steps truncated around λ and an optimal efficiency exponent $\mu_{opt}\to 1$ ($\mu_{opt}\approx 1.3$), corresponding to a nearly ballistic regime of long steps, seen in Fig. 8(a). In contrast, in the nondestructive case, Fig. 8(b), we again observe the optimal strategy for μ around 2 (in fact, $\mu_{opt}\approx 1.9$). But now, in the interval $1<\mu\leq 2$, we no longer find a vanishing efficiency for the PBC and HCB cases. Actually, in this regime the difference between the boundary conditions is negligible.

In regime III ($1<\lambda/\lambda_0<10$), one has $\mu_{opt}\to 1$ in both destructive and nondestructive cases. In this case, practically the only situations where the walker will not find a target site in a single step is if by choosing a step length from the probability distribution (1), it sorts a value $\ell_j<\lambda$. The way to

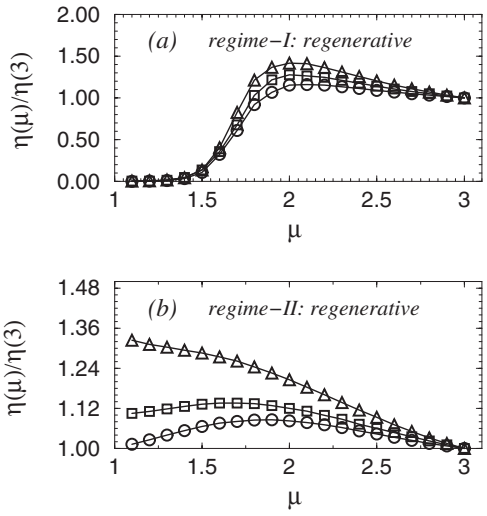

FIG. 9. The scaled efficiency $\eta(\mu)/\eta(3)$ versus μ, for the regenerative search and parameters as in the main text, corresponding to (a) regime I and (b) regime II. The recovering times are $\tau=5\times10^{-3}\lambda$ (circles), $\tau=25\times10^{-3}\lambda$ (squares), and $\tau=125\times10^{-3}\lambda$ (triangles).

avoid it is simply making μ small (close to 1), so diminishing the probability of too short step lengths ℓ_j. This case is treated analytically in the next section. Obviously, in regime-IV ($\lambda/\lambda_0\approx1$) all steps are truncated, leading to the very trivial case of a constant $\eta(\mu)$.

Finally, we consider the regenerative search; i.e., once found, the target site becomes unavailable during a certain τ, being "regenerated" and again available for the searcher after this recovering time. Of course, $\tau=0$ and $\tau\to\infty$ correspond to the nondestructive and destructive limits, respectively. For the walker always moving with a constant unitary velocity, τ can be parametrized by λ. We consider in Fig. 9 three examples $\tau=5\times10^{-3}\lambda$, $\tau=25\times10^{-3}\lambda$, and $\tau=125\times10^{-3}\lambda$. We also assume PBC and the parameters values $r_v=1$, $n_0=4\times10^6$, $n_t=10^3$, $n_d=10^3$, $\lambda/\lambda_0=1331.3$, and $L=10^5\lambda$—i.e., regime I [Fig. 9(a)]—and $r_v=1$, $n_0=4\times10^6$, $n_t=8\times10^3$, $n_d=10^4$, $\lambda/\lambda_0=153.6$, and $L=10^5\lambda$, thus belonging to regime II [Fig. 9(b)]. For the PBC and regime I, the destructive and nondestructive search efficiencies shown in Fig. 7 are qualitatively similar. It explains why in Fig. 9(a) we see no important difference in $\eta(\mu)$ for the three values for τ. However, for regime II in Fig. 9(b), as τ increases, we observe a transition of the $\eta\times\mu$ shape, from a nondestructive to a destructive behavior (compare to Fig. 8).

We present a summary of the optimal values for μ, for all situations discussed in this section, in Table II.

D. Analytical treatment of the lattice problem

The random search efficiency defined in Sec. II B can be written as

$$\eta=\frac{P}{N_s\langle\ell\rangle}, \tag{3}$$

where N_s is the mean number of steps taken between two sites and $\langle\ell\rangle$ is the mean step length of a single step. Thus, their product gives the distance traveled between two successively found sites. Here note that by a site we mean any element in the lattice that truncates the walker steps—i.e., either a target or a defect. To take into account the difference between them, we introduce the quantity P, which can be interpreted as the average probability of a sought object to be contained in a given found site. For a search with no defects, one just can set $P=1$ (a site always has a searched object), but in the present case a different choice is in order, as we discuss below. This is the essence of our mean-field-like approximation. We treat targets sites and defects alike, so we can use many of previous results in the literature [9,47,48]. However, their different contributions to η are computed in terms of their relative densities in the lattice. This simple picture makes explicitly how the defects contribute negatively to the efficiency.

Using rigorous calculations and scale analysis, it has been shown that [47,48]

$$N_s=\left(\frac{\lambda}{\lambda_0}\right)^{(1-\mu)/\Gamma}. \tag{4}$$

For $\Gamma=1$ we have the destructive and for $\Gamma=2$ the nondestructive cases. An arbitrary value $1<\Gamma<2$ interpolates between these two extreme cases, corresponding to a regenerative search, where the target sites recover after a certain time τ (how Γ is associated to such τ is discussed, for instance, in Ref. [48]).

The high probability of truncation of large steps ($\ell_j>\lambda$, for λ a kind of mean free path discussed in Sec. III A) allows one to write $\langle\ell\rangle$ as the usual first moment of the distribution

TABLE II. The optimal exponents $\mu=\mu_{opt}$ that lead to search optimization for the different situations discussed.

Regime	Boundary Condition	Destructive Search	Nondestructive Search	Regenerative Search
I	PBC	$\mu_{opt}\approx2.0$	$\mu_{opt}\approx2.0$	$\mu_{opt}\approx2.0$
I	HBC	$\mu_{opt}\approx1.8$	$\mu_{opt}\approx2.0$	$1.8<\mu_{opt}<2.0$
I	WBC	$\mu_{opt}\approx1.4$	$\mu_{opt}\approx2.0$	$1.5<\mu_{opt}<2.0$
II	Any	$\mu_{opt}\approx1.3$	$\mu_{opt}\approx1.9$	$1.0<\mu_{opt}<2.0$
III	Any	$\mu_{opt}\to1.0$	$\mu_{opt}\to1.0$	$\mu_{opt}\to1.0$
IV	Any	All equivalent	All equivalent	All equivalent

$P(\ell)$ in Eq. (1), but with an appropriate approximation for the corresponding integral, namely [9] (see also Ref. [46]),

$$\langle \ell \rangle \equiv \frac{\int_{\lambda_0}^{\lambda} \ell^{1-\mu} d\ell + \int_{\lambda}^{\infty} \lambda \ell^{-\mu} d\ell}{\int_{\lambda_0}^{\infty} \ell^{-\mu} d\ell}. \tag{5}$$

The limits λ_0 and λ of Eq. (5) relate the truncation of the steps to the properties of the search space. In particular, in environments where truncations are determined only by the density of target sites, ρ_t, and by the detection abilities (given by r_v), one has

$$\lambda_0 \equiv r_v, \quad \lambda \equiv \frac{1}{2 r_v \rho_t} = \lambda_t. \tag{6}$$

On the other hand, in environments with defects only, then $\lambda_0 = s = 1$ and $\lambda = \lambda_d$. Our aim next is to define λ and λ_0 for an arbitrary defective lattice, so as to assign Eq. (5) to the average step length of a walk through a regular background space filled both with target sites and defects.

Such a definition must distinguish and reflect the truncation due exclusively to the finding of target sites in the absence of defects (i.e., $\lambda = \lambda_t$ when $\rho_d = 0$) versus truncation due exclusively to the presence of defects in the absence of target sites ($\lambda = \lambda_d$ if $\rho_t = 0$). Thus, from such limit cases, the above results for λ_0, and from the fact that $\rho_d = 0 \Rightarrow \lambda_d \to \infty$ and $\rho_t = 0 \Rightarrow \lambda_t \to \infty$, we should expect

$$\lim_{\lambda_d \to \infty} \left(\frac{\lambda_0}{\lambda} \right) = \frac{r_v}{\lambda_t}, \quad \lim_{\lambda_t \to \infty} \left(\frac{\lambda_0}{\lambda} \right) = \frac{1}{\lambda_d}. \tag{7}$$

Since in our mean-field-like approximation we consider that the partial densities of targets and defects (which go with the inverse of the corresponding free mean paths) are additive, then a simple expression satisfying Eq. (7) can be written as

$$\frac{\lambda_0}{\lambda} = \frac{r_v}{\lambda_t} + \frac{1}{\lambda_d}. \tag{8}$$

Knowledge of either λ or λ_0 thus determines the other parameter in Eq. (8). Furthermore, we have that $\rho \sim 1/\lambda$ where $\rho = \rho_t + \rho_f$, so

$$\frac{1}{\lambda} = \frac{1}{\lambda_t} + \frac{1}{\lambda_d}, \tag{9}$$

where $\lambda_t = n_0/(2 r_v n_t)$ and $\lambda_d = n_0/n_d$. By solving Eqs. (8) and (9), we obtain

$$\lambda_0 = \frac{r_v + \lambda_t/\lambda_d}{1 + \lambda_t/\lambda_d}. \tag{10}$$

Observe that $1 \leq \lambda_0 \leq r_v$ arises as a consequence of the conditions in Eq. (7). It is also convenient to express λ and λ_0 as functions of the "control" parameters r_v, n_0, n_t, and n_d or [49]

$$\lambda_0 \equiv \frac{n_d + 2 r_v^2 n_t}{n_d + 2 r_v n_t}, \quad \lambda \equiv \frac{n_0}{n_d + 2 r_v n_t}. \tag{11}$$

Finally, we discuss the appropriate definition of P, the quantity which gives the relative contributions of target and defects to the efficiency. Actually, in terms of the step truncation dynamics, the target sites and defects play, qualitatively speaking, similar roles. It is seen, for instance, in the results presented in Sec. III A. But of course, targets and defects are different in two very relevant aspects. The obvious one is that if a step halts due to a defect, contrary when it does due to a target site, the walker "gains" nothing and such truncation contributes negatively for the efficiency (locomotion without finding the object). The second is that since a step is truncated only if the defect is blocking the way (i.e., no lateral defects can stops the movement, opposite to the case of target sites), then effectively the defects have a lower truncation power. Therefore, we can think about the defect as a "fake" target site, which is also harder to find. So, with this picture in mind, we can write $P = [1 + (f \rho_d)/\rho_t]^{-1}$. The term f weights the relative truncation power of defects and target sites. It should depend on r_v, the detection radius of defects—which is simply the lattice parameter s—and the connectively of the lattice. Based on a straightforward geometric reasoning, one realizes that $f \sim s/((k-1) r_v)$, with $k = 6$ for our triangular lattice.

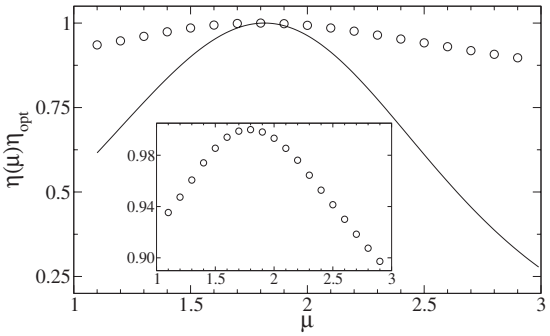

FIG. 10. $\eta(\mu)$, normalized by the maximum efficiency η_{opt}, for the nondestructive search and parameters as in the main text. The analytic model and the numerical simulations (circles) do not fall off from their peaks at the same rates. However, from a blowup of the latter (inset), it becomes clear that both cases have a very similar shape behavior.

Considering all these results in the efficiency formula, Eq. (3), we end up with a type of "mean-field" model to describe our defective lattice random search problem [50].

The qualitative agreement between the analytical η and the numerical simulation is shown in Fig. 10, for a nondestructive search and regime II, where the differences between the boundary conditions are not relevant. We consider the parameters values $r_v = 5$, $n_0 = 2.5 \times 10^7$, $n_t = 5 \times 10^3$, $n_d = 5 \times 10^3$, $\lambda/\lambda_0 = 98.04$, and $L = 10^5 \lambda$. Thus, d is around λ (see regime II in Table I) and correspond to the same truncation imposed on the analytical expression for $\langle \ell \rangle$, Eq. (5). We see that the normalized curves are very similar, having a same shape behavior and presenting the maximum at the same value of μ. But they do not fit to a same relative scale; the analytic model decays from the peak faster than the numerical simulation. To a great extent the differences in Fig. 10 can be understood from the following. Although our approximations properly handle the way defects truncate the walk, there is an extra factor not included in the model. In fact, the defects introduce a certain number of "holes" in the lattice

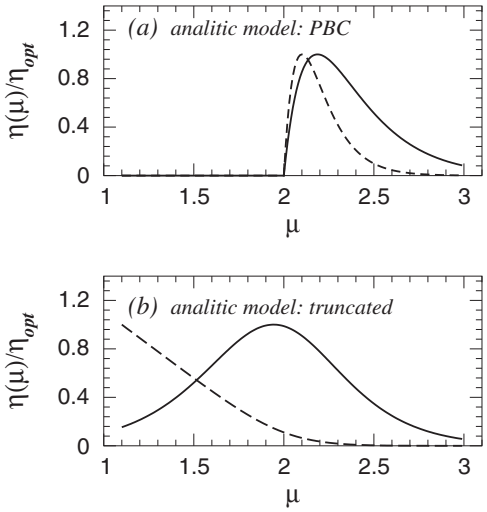

FIG. 11. Analytic normalized efficiency $\eta(\mu)/\eta_{opt}$, as a function of μ, for the nondestructive (solid) and destructive (dashed) curves in regime I. The parameters are given in the main text. (a) A lattice with the PBC, for which $\lambda \to \infty$ in Eq. (5). (b) A "truncated" lattice, for which λ in Eq. (5) is taken from its actual numerical value, given by Eq. (11).

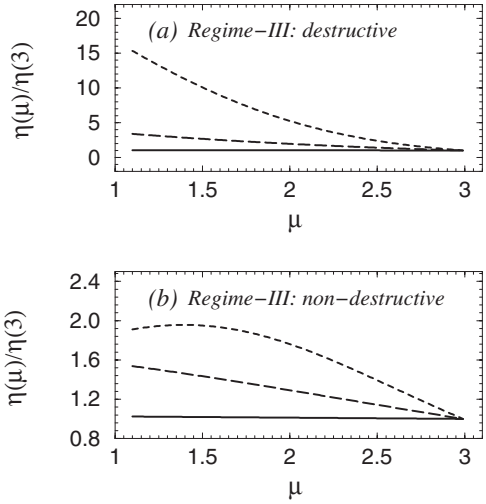

FIG. 12. Analytic $\eta(\mu)/\eta(3) \times \mu$ for regime III, parameters as in the main text, and (a) destructive and (b) nondestructive cases. The curves correspond to $r_v=6$ (short-dashed curve), $r_v=12$ (long-dashed curve), and $r_v=18$ (solid curve).

(see Fig. 2). So a pure Euclidian metric (at any scale and direction), true for continuous spaces and perfect lattices and implicitly assumed in the analytic expressions, does not completely hold in defective lattices. This inhomogeneity, correctly captured in the simulations, makes the efficiency less sensitive to changes in the step lengths distribution (controlled by μ). Probably, it can be fixed by the inclusion of a necessary numerical factor, associated with the lattice topology and defects density, multiplying λ/λ_0 in Eq. (4). We should mention that presently we are studying such problem and the results will be reported in the due course.

Another aspect that the model can reproduce well, illustrating a key role played by the boundary conditions allied to the target densities, is the particular behavior of the PBC in regime I, for which when $\mu \to 1$ the efficiency $\eta(\mu)$ goes to zero in both destructive and nondestructive searches. But for this, some care is necessary to properly define λ in Eq. (5). For example, let us consider the parameters $r_v=1$, $n_0=2.5 \times 10^7$, $n_t=10^3$, and $n_d=10^3$, so that the $\lambda/\lambda_0=8334$ is a relatively large value. However, since here we want to explicitly see the influence of the loops, we just allow arbitrarily long step lengths ℓ_j; i.e., no upper cutoff is assumed. Hence, we set, in Eq. (5), $\lambda \to \infty$. In this case, the curves in Fig. 11(a), destructive and nondestructive searches, show an abruptly vanishing efficiency for $\mu < 2$. Of course, this sharp transition is an artifact of assuming an infinite λ. By considering a very large but finite λ, we would also observe a rapid decay, but with no divergence for $d\eta(\mu)/d\mu$. These results are in agreement with Fig. 7. On the other hand, in Fig. 11(b) we use exactly the same parameters, but take the actual value of λ in Eq. (5), which for such reason we call "truncated" lattice. In this case, we see that the results do not agree with those observed for the PBC lattice. They are similar to what should be expected for a continuous environment search [9,47,48].

As a last case, we consider regime III, whose qualitative behavior, already discussed in Sec. III C, is simple to predict but demanding to simulate. Indeed, since the density of target or defects is high, the step lengths truncations do occur quite frequently. So, to calculate any relevant quantity, a lot of different realizations are necessary for satisfactory averages. Hence, in this situation the analytical model is very appropriate. For the plots of $\eta(\mu)/\eta(3)$ in Fig. 12, we assume $n_0=4 \times 10^6$, $n_t=6 \times 10^3$, and $n_d=10^4$ and three different values for r_v: namely, 6, 12, and 18. They correspond, respectively, to $\lambda/\lambda_0=9.05$, $\lambda/\lambda_0=2.30$, and $\lambda/\lambda_0=1.03$. Note that $\mu_{opt} \to 1$, indicating that the high truncation rate favors always to choose long step lengths (see Sec. III C). From the curves we also see that for increasing values of r_v (i.e., increasing of the detection power), the relative advantage of a Lévy process ($\mu < 3$) over a Brownian strategy ($\mu=3$) diminishes, an intuitive but nonetheless important fact for search optimization.

IV. REMARKS AND CONCLUSION

In the present exploratory contribution we have discussed many aspects influencing the random search in defective lattice networks, focusing on the triangular structure case. The defects were created through random elimination of a fraction χ of the original nodes. We have studied the efficiency function $\eta(\mu)$, obtaining the values of $\mu=\mu_{opt}$ that lead to optimal strategies. We have found that the shapes of the efficiency curves $\eta(\mu)$ and the values of μ_{opt} are strongly dependent on the density of target sites and defects, the boundary conditions, and the type of search process—i.e., whether destructive, nondestructive, or regenerative. We can summarize our main results as follows: (i) for any strategy effectively to improve the random search efficiency, the number of defects cannot be too high (see also below); (ii) for low target concentrations, the specific boundary conditions are very important in defining the behavior of $\eta(\mu)$; and (iii)

$\eta(\mu)$ for nondestructive and destructive searches present some similarities at low densities of targets.

Next, final remarks are in order. As we have seen, a key aspect in determining the dynamics of the search is related to the frequency in which the steps lengths ℓ_j are truncated. It takes place each time the walker finds a target site or hits a defect. Considering their densities, parametrized by the effective mean free path λ, Eq. (11), we have that for very large λ's, low density of targets and defects (regime I), the specific type of boundary conditions plays an important role for smaller values of μ. This, however, is not the case for $\mu > 2$, since then the average step lengths are smaller and thus the walker does not reach the lattice boundary frequently. Furthermore, for shorter λ—i.e., regimes II and III (regime IV is trivial)—the boundary conditions are also not relevant. Indeed, in these situations $\eta(\mu)$ for a same parameter set but different boundary conditions collapse to a single behavior (see Fig. 8).

We can draw a parallel with the perfect lattice case: Reference [32] discussed one square and two triangular lattices (differing by how much of the lattice nodes a single huge step could visit), all with the PBC. The calculated efficiency curves for such regular lattices showed that in general the $\eta(\mu)$'s were higher for the more ergodic lattices (i.e., those where the walker more easily could scan the search space). For defective lattices, we see exactly the same behavior (e.g., Fig. 7). But the difference is that here it is the boundary conditions which determine the performance of the scan mechanisms.

Furthermore, regarding the shape of the curves, for regimes I and II all the lattices in Ref. [32] present an efficiency which is qualitatively similar to our cases of PBC and HBC, both for destructive and nondestructive searches. The exception is the RBC in regime I, because as already mentioned it always truncates the flight at the borders of the lattice and therefore no looping can take place. For regime III there are no simulations for comparison, but one also can expect qualitative agreement.

An interesting aspect observed for regular as well as for fragmented lattices in the cases of PBC and HBC is that destructive and nondestructive searches present similarities which are absent in a continuous space search. But of course, this is true only in regime I. For the other regimes, lattices and continuous spaces somewhat resemble each other, which becomes evident if one can compare Figs. 8(a), 8(b), 9(b), and 11(b) with the results in the Refs. [9,48].

We have also analyzed how the defects influence the search efficiency. Intuitively speaking, defects should decrease $\eta(\mu)$. Indeed, many steps are truncated due to their presence. Such locomotion is just noise, spurious, increasing the total distance traveled without finding extra target sites. From the calculations in Sec. III A we have found that when the defects density χ is higher than 10%, the number of truncated steps increases very rapidly. Hence, the particular random search strategy (the chosen μ) starts not to be very important for the efficiency outcome. On the other hand, for lower χ's, the dynamics of truncation due to defects and target sites are very similar. Thus, we can think about a defect as a target site, but with no target object in it. In this case, the presence of defects is just like rescaling the target sites density. From such reasoning—crucial for understanding qualitatively the differences and similarities between searches undertaken on regular lattices and defective lattices—we have been able to develop an analytical model, leading to good qualitative agreement with the numerical simulations.

The above discussion relates to an important issue. What exactly is the threshold for χ such that above it random search optimization may no longer be possible? This question bears the relevant point of how robust is a given lattice to defects regarding efficient searching, a problem that will be the focus of a future contribution.

As the last observation we comment that very recent empirical studies of animal locomotion [51] have uncovered an apparent paradox concerning Lévy flights: why do certain organisms not perform Lévy motion known to optimize the foraging process? In the present study we have found (in the context of lattices landscapes) that depending on different factors, (i) the boundary conditions, (ii) the presence of defects, (iii) the density of target sites, and (iv) the detection power (here represented by the value of r_v); the relative advantage of Lévy flights strategies is drastically diminished compared to other strategies, such as ballistic or pure Brownian motion. It indicates that the necessary conditions (see, e.g., the discussion in Ref. [9]) for a Lévy random search strategy to lead to the highest encounter rates may not be fulfilled depending on the above (or other) environmental factors—thus, a possible explanation for the above-posed question.

ACKNOWLEDGMENTS

We would like to thank Carlos Carvalho for computational support and CNPq-Edital Universal, Finep/CT-Infra, F. Araucaria, FACEPE, and FAPEAL for funding. The authors also acknowledge support from CNPq.

[1] D. W. Stephens and J. R. Krebs, *Foraging Theory* (Princeton University Press, Princeton, 1987).
[2] *Foraging Behavior*, edited by A. C. Kamil, J. R. Drebs, and H. R. Pulliam (Plenum Press, New York, 1987).
[3] M. F. Shlesinger and J. Klafter, in *On Growth and Form*, edited by H. E. Stanley and N. Ostrowsky (Nijhoff, Dordrecht, 1986).
[4] M. Levandowsky, J. Klafter, and B. S. Whilte, Bull. Mar. Sci. **43**, 758 (1988).
[5] B. J. Cole, Anim. Behav. **50**, 1317 (1995).
[6] P. Nonacs and L. M. Lill, Oikos **67**, 371 (1993).
[7] F. L. Schuster and M. Levandowsky, J. Eukaryot. Microbiol. **43**, 150 (1996).
[8] G. M. Viswanathan, V. Afanasyev, S. V. Buldyrev, E. J. Murphy, P. A. Prince, and H. E. Stanley, Nature (London) **381**, 413 (1996).

[9] G. M. Viswanathan, S. V. Buldyrev, S. Halvin, M. G. E. da Luz, E. P. Raposo, and H. E. Stanley, Nature (London) **401**, 911 (1999).
[10] S. V. Buldyrev, M. Gitterman, S. Havlin, A. Y. Kazakov, M. G. E. da Luz, E. P. Raposo, and H. E. Stanley, Physica A **302**, 148 (2001).
[11] G. M. Viswanathan, F. Bartumeus, S. V. Buldyrev, J. Catalan, U. L. Fulco, S. Havlin, M. G. E. da Luz, M. L. Lyra, E. P. Raposo, and H. E. Stanley, Physica A **314**, 208 (2002).
[12] F. Bartumeus, F. Peters, S. Pueyo, C. Marrase, and J. Catalan, Proc. Natl. Acad. Sci. U.S.A. **100**, 12771 (2003); F. Bartumeus, M. G. E. da Luz, G. M. Viswanathan, and J. Catalan, Ecology **86**, 3078 (2005).
[13] G. Ramos-Fernandez, J. L. Mateos, O. Miramontes, G. Cocho, H. Larralde, and B. Ayala-Orozco, Behav. Ecol. Sociobiol. **55**, 223 (2004); D. Boyer, O. Miramontes, G. Ramos-Fernandez, J. L. Mateos, and G. Cocho, Physica A **342**, 329 (2004).
[14] F. A. L. Dullien, *Porous Media—Fluid Transport and Pore Structure (Academic Press, New York, 1979); M. Sahimi, Flow and Transport in Porous Media and Fractured Rock* (VCH, Boston, 1995).
[15] C. L. Faustino, L. R. da Silva, M. G. E. da Luz, E. P. Raposo, and G. M. Viswanathan, Europhys. Lett. **77**, 30002 (2007).
[16] P. Pirolli and S. Card, in *Proceedings of the 1995 Conference on Human Factors in Computing Systems*, edited by G. C. van der Veer and C. Gale (ACM Press, New York, 1995), pp. 51–58.
[17] A. Freking, W. Kinzel, and I. Kanter, Phys. Rev. E **65**, 050903(R) (2002).
[18] A. Potapov and M. K. Ali, Phys. Rev. E **65**, 046212 (2002).
[19] D. Z. Jin and H. S. Seung, Phys. Rev. E **65**, 051922 (2002).
[20] A. Vazquez, R. P.-Satorras, and A. Vespignani, e-print arXiv:cond-mat/0206084.
[21] S. Kutten and D. Peleg, Comput. Netw. **51**, 190 (2007).
[22] J. J. Collins and C. C. Chow, Nature (London) **393**, 409 (1998); J. P. Onnela, J. Saramaki, J. Hyvonen, G. Szabo, M. A. de Menezes, K. Kaski, A. L. Barabasi, and J. Kertesz, New J. Phys. **9**, 179 (2007).
[23] L. A. Adamic, R. M. Lukose, A. R. Puniyani, and B. A. Huberman, Phys. Rev. E **64**, 046135 (2001).
[24] R. Guimerà, A. Díaz-Guilera, F. Vega-Redondo, A. Cabrales, and A. Arenas, Phys. Rev. Lett. **89**, 248701 (2002).
[25] D. J. Watts and S. H. Strogatz, Nature (London) **393**, 440 (1998).
[26] L. A. N. Amaral, A. Scala, M. Barthelemy, and H. E. Stanley, Proc. Natl. Acad. Sci. U.S.A. **97**, 11149 (2000).
[27] R. Cohen, K. Erez, D. ben-Avraham, and S. Havlin, Phys. Rev. Lett. **85**, 4626 (2000); D. S. Callaway, M. E. J. Newman, S. H. Strogatz, and D. J. Watts, *ibid.* **85**, 5468 (2000); R. Albert, H. Jeong, and A. L. Barabasi, Nature (London) **406**, 378 (2000); P. Holme, B. J. Kim, C. N. Yoon, and S. K. Han, Phys. Rev. E **65**, 056109 (2002); G. Paul, S. Sreenivasan, S. Havlin, and H. E. Stanley, Physica A **370**, 854 (2006); S. Kutten and D. Peleg, Comput. Netw. **51**, 190 (2007).
[28] M. Barthélémy and Luís A. Nunes Amaral, Phys. Rev. Lett. **82**, 3180 (1999); A. Barrat and M. Weight, Eur. Phys. J. B **13**, 547 (2000).
[29] R. Albert, H. Jeong, and A. L. Barabasi, Nature (London) **401**, 130 (1999).
[30] J. M. Kleinberg, Nature (London) **406**, 845 (2000).
[31] S. Sreenivasan, R. Cohen, E. López, Z. Toroczkai, and H. E. Stanley, Phys. Rev. E **75**, 036105 (2007).
[32] M. C. Santos, G. M. Viswanathan, E. P. Raposo, and M. G. E. da Luz, Phys. Rev. E **72**, 046143 (2005).
[33] O. V. Kirillova, Phys. Rev. Lett. **87**, 068701 (2001); R. Lambiotte, J. Stat. Mech.: Theory Exp. (2007) P02020.
[34] B. Pagurek, N. Dawes, and R. Kaye, Lect. Notes Artif. Intell. **604**, 256 (1992).
[35] E. Cascetta and F. Russo, Transportation **24**, 271 (1997).
[36] A. L. Barabasi and Z. N. Oltvai, Nat. Rev. Genet. **5**, 101 (2004).
[37] M. L. Siegal, D. E. L. Promislow, and A. Bergman, Genetica (Dordrecht, Neth.) **129**, 83 (2007).
[38] M. F. Sykes and J. W. Essam, Phys. Rev. **133**, A310 (1964).
[39] Which is the case for relative large lattices and not too long simulation times, two conditions observed in the present work.
[40] M. F. Shlesinger, G. M. Zaslavsky, and J. Klafter, Nature (London) **363**, 31 (1993).
[41] *Lèvy Flights and Related Topics in Physics*, edited by M. F. Shlesinger, G. M. Zaslavsky, and U. Frisch (Springer, Berlin, 1995).
[42] C. Tsallis, Phys. World **10**(7), 42 (1997).
[43] C. Tsallis, S. V. F. Levy, A. M. C. Souza, and R. Maynard, Phys. Rev. Lett. **75**, 3589 (1995).
[44] C. Tsallis, S. V. F. Levy, A. M. C. Souza, and R. Maynard, Phys. Rev. Lett. **77**, 5442 (1996).
[45] S. V. Buldyrev, A. L. Goldberger, S. Havlin, C.-K. Peng, M. Simons, and H. E. Stanley, Phys. Rev. E **47**, 4514 (1993).
[46] R. N. Mantegna and H. E. Stanley, Phys. Rev. Lett. **73**, 2946 (1994).
[47] M. G. E. da Luz, S. V. Buldyrev, S. Havlin, E. P. Raposo, H. E. Stanley, and G. M. Viswanathan, Physica A **295**, 89 (2001); S. V. Buldyrev, S. Havlin, A. Y. Kazakov, M. G. E. da Luz, E. P. Raposo, H. E. Stanley, and G. M. Viswanathan, Phys. Rev. E **64**, 041108 (2001).
[48] E. P. Raposo, S. V. Buldyrev, M. G. E. da Luz, M. C. Santos, H. E. Stanley, and G. M. Viswanathan, Phys. Rev. Lett. **91**, 240601 (2003); M. C. Santos, E. P. Raposo, G. M. Viswanathan, and M. G. E. da Luz, Europhys. Lett. **67**, 734 (2004).
[49] The simpler choice of setting λ as in Eq. (11), but to assume λ_0 arbitrary—e.g., $\lambda_0 = r_v$—does not alter qualitatively our results, as we have checked.
[50] An alternative is to notice that the mean step $\langle \ell \rangle$ in the lattice with sites and defects should be smaller than both (i) the mean step in a lattice with sites only $\langle \ell_t \rangle$ and (ii) the mean step in a lattice with defects only $\langle \ell_f \rangle$, thus leading to the definition $1/\langle \ell \rangle \equiv 1/\langle \ell_t \rangle + 1/\langle \ell_f \rangle$. We prefer to keep $\langle \ell \rangle$ defined by the integral Eq. (5) and to change the integration limits λ_0 and λ.
[51] A. M. Edwards, R. A. Phillips, N. W. Watkins, M. P. Freeman, E. J. Murphy, V. Afanasyev, S. V. Buldyrev, M. G. E. da Luz, E. P. Raposo, H. E. Stanley, and G. M. Viswanathan, Nature (London) **449**, 1044 (2007).